

HIGH STRENGTH BETA TITANIUM ALLOY FORGINGS
FOR
AIRCRAFT STRUCTURAL APPLICATIONS

C. C. Chen, Wyman-Gordon Company, Worcester, Massachusetts
J. A. Hall, TIMET Division of TMCA, Henderson, Nevada
R. R. Boyer, Boeing Company, Seattle, Washington

Introduction

When the alloy Ti-10V-2Fe-3Al (Ti-10-2-3) was first introduced [1, 2], its improved hot workability and higher fracture toughness led the alloy to be extensively evaluated as a potential cost reduction forging alloy alternative to the popular Ti-6Al-4V alloy [3-5]. In the early developmental efforts, the bulk of technical interest focused on the low and intermediate strength conditions where high fracture toughness forgings could be produced [3,4]. Because all properties of the low and intermediate strength versions were adequate and relatively insensitive to considerable compositional inhomogeneity, little attention was paid to the optimization of ingot production and processing variables for producing the forgings.

Recent interest at Boeing for applications of titanium at high strength (1242 MPa or 180 Ksi ultimate tensile strength) revived serious consideration of the Ti-10-2-3 alloy in its high strength condition. The use of a titanium alloy at the 1242-1380 MPa (180-200 ksi) strength level could compete with high strength steels and Ti-6-4 alloy for aerospace applications. Although the early results of the forgings obtained from laboratory scale ingots demonstrated that the alloy is suited for high strength applications [4], initial evaluation of the alloy's capability to reproducibly achieve 1242 MPa (180 Ksi) UTS with fracture toughness of 44 MPa \sqrt{m} (40 ksi \sqrt{in}) met with mixed success. Considerable effort was then carried out by the ingot producer and the forging suppliers to develop the manufacturing capability.

The primary objective of this paper is to present the manufacturing techniques for the melting practices and the forging methods required for manufacturing high strength Ti-10-2-3 forgings. Emphasis is made on the controls over chemistry uniformity during melting, and the forging sequencing necessary to produce the strength-ductility-toughness property combinations suitable for advanced airframe applications. The minimum property goals of this program were 1242 MPa (180 ksi) ultimate tensile strength, 4% elongation, and 44 MPa \sqrt{m} (40 ksi \sqrt{in}) fracture toughness.

Melting Development

Because of the high alloy content of β -titanium alloys, control over chemistry uniformity during consumable arc melting is a difficult task, particularly when producing large production-size ingots. It was learned that the primary problem for Ti-10-2-3 alloy was compositional segregation, on both a macro- and micro-scale, with iron being the most severe. The magnitude of the macrosegregation was sufficient to produce significant changes in the macrostructure, greatly increasing property scatter, and the microsegregation produced β -flecks, which adversely affected ductility of the forgings. However, by proper manipulation of the melting parameters, ingots of Ti-10-2-3 were produced having minimal macro- and microsegregation, thereby enabling the production of the uniform microstructure in the final forge product.

Macrosegregation

Two classes of liquid-solid phase diagrams can result from alloying additions for binary Ti-X alloys in the titanium rich region: the melting point suppressors and the melting point raisers. The term $k = C_s/C_l$, the solid/liquid compositional partitioning ratio, reflects the sense of the melting point change, describes the compositional width of the solid-liquid phase region, and thereby indicates the solute partitioning tendency. With very slow liquid \rightarrow solid transformations, where equilibrium conditions would prevail, k can be determined from the equilibrium phase diagram. However, seldom are equilibrium conditions realized since a solid-liquid interface advancing into the liquid creates nonequilibrium conditions such that k effectively ranges between the equilibrium value, k_o , and unity [6]. The influence that freezing conditions have on k in binary systems solidifying via an advancing planar interface can be described as (6):

$$k = \frac{1}{1 + \left(\frac{1-k_o}{k_o}\right) \exp\left(\frac{-v\delta}{D}\right)} \quad \text{(Equation 1)}$$

Here v is the freezing velocity of the solid-liquid interface, D is the effective diffusivity of the solute in the liquid near the interface and δ is the thickness of the diffusion layer in the liquid.

From Equation 1 and Figure 1, which describe a compositional profile at the liquid-solid interface, it is apparent that any kind of disturbance in the liquid layer at the interface is likely to modify both the layer thickness as well as the effective diffusivity. The partitioning ratio also depends strongly on the velocity of the solid-liquid interface. A smaller value of δ and v or a larger D will effectively reduce the value of k . On the other hand, increasing v or δ and decreasing D will have the opposite effect of increasing k . However, the overall effect of manipulating boundary layer conditions on solute partitioning ratio can be related to the dimensionless parameter $v\delta/D = \Delta$. As Δ increases, k increases.

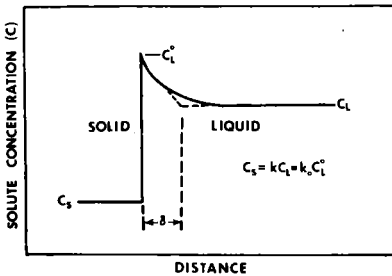


Figure 1 Solute distribution near a solid/liquid interface advancing into the liquid for conditions where $k < 1$.

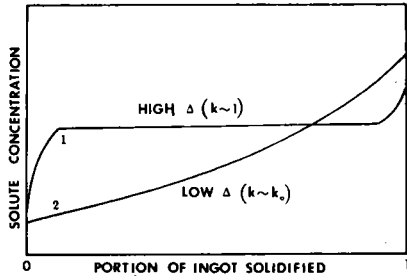


Figure 2 Schematic, exaggerated, of solute distribution along a directionally solidified ingot for extremes of the operating parameter, Δ .

The consequences of increasing or decreasing k in a directionally solidifying system, as encountered in a consumable vacuum arc melting situation when a planar interface persists, is described by Figure 2.

It can be seen by the above discussion that macrosegregation patterns in directionally solidified vacuum arc remelted ingots, where the electrode

is of constant and uniform composition along its length, can be dramatically influenced by manipulating the components (v , δ , D) of Δ .

Any mechanical means of increasing D will also serve to decrease δ . Creating liquid pool motion at the solid-liquid interface will serve to decrease Δ causing the pattern of macrosegregation to tend toward Curve 2 in Figure 2. A quiescent pool will tend toward a macrosegregation pattern like that of Curve 1, a situation sought and approached during zone refining. With appropriate electrode formulation, compensation for the end effects seen in Curve 1 can be made, and this situation would appear most appropriate for producing homogeneous ingots on a macro scale. This is, minimum liquid pool stirring and maximum freezing velocity. Thus, the ramifications of Equation 1 and Figure 2 point toward the conditions necessary to avoid macrosegregation by suitable compensation in the initial electrode formulation.

Microsegregation

The microstructural phenomenon known as beta flecks is a well-known feature of vacuum consumable arc-melted titanium alloys containing β -phase stabilizers which also tend to partition rather strongly between the solid and liquid states during solidification [7]. Beta flecks are described as localized regions of abnormally low β -transus temperature and are seen as regions void of or lean in α -phase. The flecks tend to exhibit quite different properties. Methods for minimizing these micro-inhomogeneities became obvious when consideration was given to those factors of the alloy formulation and the melting/solidification conditions imposed during ingot production. Solidification conditions, particularly those associated with an advancing solid interface, are key factors in the understanding of alloy segregation in general, and must be known in order to design a manufacturing method which will minimize associated problems of microsegregation. This is particularly important in order to achieve an optimized balance of strength and ductility properties of the alloy forgings at high strengths.

Microsegregation, as it manifests itself in the Ti-10-2-3 alloy or any titanium alloy, has been previously discussed in general terms [7, 8]. These papers described a microsegregation tendency parameter, T , having the units of absolute temperature, which indicates an alloy's inherent tendency to produce microsegregation associated with aspects of constitutional supercooling such as dendrites and cellular growth [9]. Such a description of microsegregation tendencies in multicomponent titanium alloys is given below:

$$T = \sum_{i=1}^n -M_i C_i \left(\frac{1-k_i}{k_i} \right) \quad (\text{Equation 2})$$

Here k_i is the ratio of solute concentration in the solid to that in the liquid beyond the diffusion zone, M_i is the slope of the liquidus curve and C_i is the bulk solute composition of component i in the liquid for an n component alloy.

In consumable vacuum arc melted ingots [8], the values for the segregation temperature, T , were calculated with Equation 2. It was found that the alloys with this parameter in excess of about 40°K exhibit extensive β flecking tendencies. By utilizing the binary phase diagrams, the compositional dependence of T for several common titanium alloying elements was determined [8]. From these results, the T value for Ti-10-2-3 is estimated

to be 66.5°K by assuming as was done that there exists no interaction between the alloying elements. This value is in excess of the level estimated to be critical for flecking tendencies and the appearance of β -flecks in Ti-10-2-3 is therefore not surprising.

The operating parameters of solidification which relate to the conditions for a voiding dendritic or cellular freezing and promoting a planar solidification front are described below [7]:

$$\frac{G_L D_L}{v} > -MC \left(\frac{1-k}{k} \right) \quad (\text{Equation 3})$$

Here, G_L is the thermal gradient in the liquid at the liquid-solid interface, D_L is the effective solute diffusivity for the liquid in the diffusion zone, and v is the velocity of the solid interface. When the inequality of Equation 3 holds, the solidification front is planar, not dendritic. This parameter then relates to conditions which avoid dendritic freezing and hence avoid the associated β -flecks.

Forging Parameters and Heat Treatments

From a production standpoint, the achievable property combinations at high strengths are also critically dependent on the forging and heat treatments applied. As titanium alloys begin to reach their maximum strength capability for production forgings, close control of both processing variables and resultant microstructures becomes necessary for producing forgings with optimum properties [10, 11].

Forging Sequence/Microstructure/Property Relationship

From a metallurgical standpoint, forge processes with extensive $(\alpha+\beta)$ deformations are generally applied in order to refine microstructures to assure uniformly high ductility accompanying the desired strength throughout the forging. However, the resultant well-defined globular- α morphology has an adverse influence on fracture toughness. On the other hand, the development of platelet α -particles resulting from beta processing appear to reduce ductility while concurrently improving fracture toughness. Figures 3a and 3b illustrate the influence of $(\alpha+\beta)$ work on fracture toughness and tensile ductility respectively. The variations of α -phase morphology influenced by the degree of forging in the two-phase region, as discussed above, are evident. It is seen that tight control of the forging sequences is necessary to achieve the present goals for strength, toughness, and ductility combinations.

Figure 4a presents strength and toughness properties of forgings produced from production ingots including early heats for which melting practices had not been optimized. Several forging sequences were used and no good correlations between process and properties were possible. Much of this failing can be attributed to the ingot inhomogeneities discussed in this paper and which have been corrected. Once compositional uniformity was obtained, forgings were significantly improved by specific TMP conditions. It was observed that significant improvements in the fracture toughness were achieved by the forging sequence of β -blocking with an $(\alpha+\beta)$ finish of about 5 to 20%. The consequence of higher amounts of $(\alpha+\beta)$ forging was seen in Figures 3a and 3b to be reduced toughness and increased ductility. The inserted data band in Figure 4a is that obtained from the optimized processing, including melting, forging, and heat treatment.

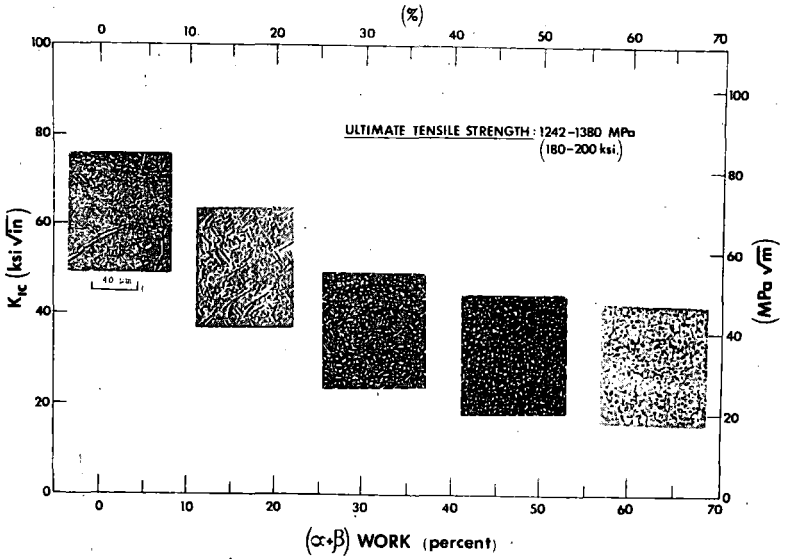


Figure 3a Effect of alpha-beta work on fracture toughness of high strength Ti-10V-2Fe-3Al alloy forging

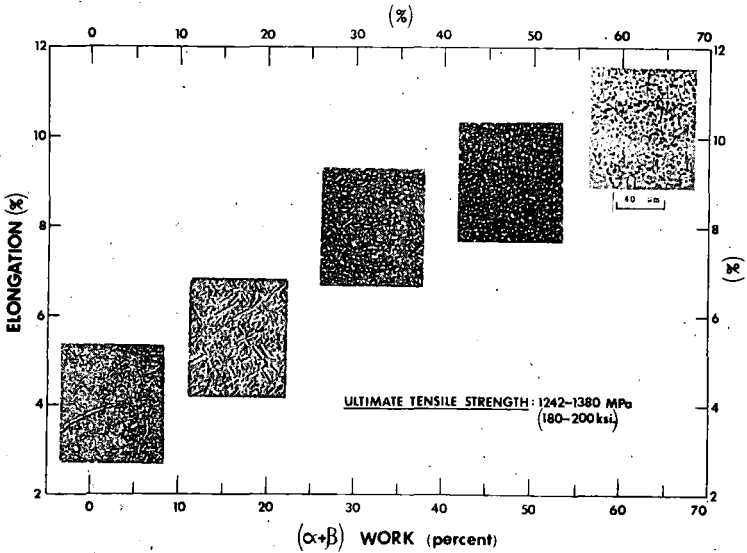


Figure 3b Effect of alpha-beta work on tensile ductility of high strength Ti-10V-2Fe-3Al alloy forging

Optimization of Heat Treatments

For the ultimate tensile strength goal of 1242 MPa (180 ksi) it was necessary to solution treat, water quench and age. However, a double solution treatment followed by aging was developed in this program for producing

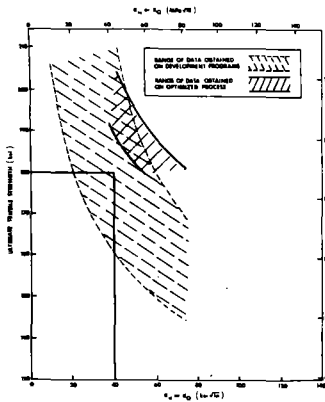


Figure 4a Comparison of strength-fracture toughness relationships for high strength Ti-10V-2Fe-3Al alloy forgings produced from development programs and from optimized process

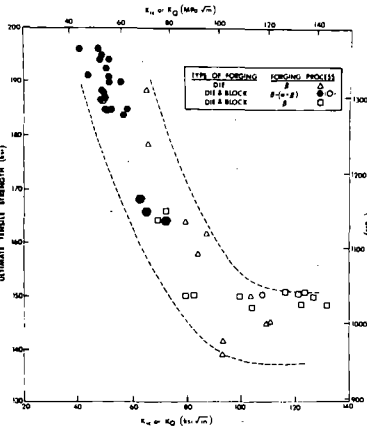


Figure 4b Achievable strength-fracture toughness combinations for Ti-10V-2Fe-3Al alloy forgings.

the forgings with adequate strength-toughness-ductility combinations. Such a triplex heat treatment was 780C/2 hours/air cool + 774C/2 hours/W.Q. + 510C/8 hours (1435F/2 hours/A.C. + 1425F/2 hours/W.Q. + 950F/8 hours/A.C.)

The double solution treatment was introduced in an effort to combine the increased ductility trend observed with primary globular- α morphology and the higher toughness associated with the primary acicular or lenticular- α . The α -phase in the cooled β -forging consisted of acicular and grain boundary forms and while high toughness might be expected, a low ductility would also be obtained. The limited ($\alpha+\beta$) finish forging would serve to partially break up the grain boundary alpha and reduce the aspect ratio of the primary acicular- α . The first solution treatment takes the product of the slightly ($\alpha+\beta$) worked structure, and normalizes the microstructure by an exposure close to; but below, the β -transus. The short exposure is necessary to assure that the primary- α retains most of its acicular morphology. Air cooling allows the alpha to grow somewhat, retaining its initial configuration. The second solution treatment which must be performed close to, but below, the temperature of the first allows some globular- α to form and the water quench establishes metastable- β for subsequent aging to establish the hardenability. This solution treatment fixes the primary alpha:beta ratio.

An increase in the first solution temperature may have a beneficial effect on the fracture toughness, but the maximum temperature is limited by the temperature at which the β -flecks occur, emphasizing the need for good micro-homogeneity. Slight variations in the solution treat temperature is often necessary, depending on the section-thickness of the forgings, and the minimum β -transus of the material. Since the second solution before quenching has an important effect on the strength capability, the heat-transfer and the delay time from the furnace to the quench tank must be considered before quenching various section thicknesses for a given structural component forging.

Solution temperature, quench rate, and aging temperature all influence the aging response of the alloy forgings. Experience on Ti-10-2-3 alloy

forgings also indicated that the fracture toughness of the alloy forgings could be improved by increasing the alloy temperature. At the 1242-1380 MPa (180-200 ksi) strength level, it was found that averaging at 480C (900F) or higher produced better toughness and ductility values as well as property uniformity than underaged conditions. The age hardening mechanism is due to precipitation of fine, noncoherent alphas.

Reproducibility of Established Forging and Heat Treating Practice

A comprehensive properties evaluation was made on forgings produced by three different forging sources, each of which was done in production facilities. Figure 4b presents the range of achievable strength-fracture toughness combinations for the Ti-10-2-3 alloy forgings illustrating particularly excellent strength-toughness combinations of the high strength forgings obtained from β -blocking plus $(\alpha+\beta)$ finish forging. These data were generated from three separate heats of material and include both press and hammer forging processes. The forgings ranged from about 45 kg (100 pounds) to 114 kg (250 pounds) cut weight and included thickness variations from about 12.7 to 82.5 mm (0.5 to 3.25 inches). Most of the data was obtained using triplex heat treatments (double solution treat and age), although some of the material was simply solution treated (732C/2 hours/W.Q.) and aged (496C/8 hours).

Very extensive testing was performed on Boeing 747 Lower Link Fitting forgings (Figure 5a) supplied by Wyman-Gordon; this forging is currently made of Ti-6-4 alloy. This forging is 1500 mm (59 inches) in length, 406 mm (16 inches) in width, 0.4 m² (611 square inches) in plan view where the web thickness ranges from 25 mm (1 inch) to 82 mm (3.25 inch). Note that this forging includes those features of typical production spar and fitting forgings, and also offers adequate forging size and thickness to provide abundant material for the testing program. The forgings were produced by combined β -blocking and $(\alpha+\beta)$ finish forging, with the percent $(\alpha+\beta)$ deformation controlled to within 20% reduction. The heat treatment applied here was triplex heat-treatment.

The microstructural features of the forgings are given in Figure 5b at different locations and orientations; excellent macro- and microstructural uniformities are observable. Note that the forging contains 5 to 10% primary α with both acicular and globular- α morphologies seen.

Results of Other Design Properties and Cost Considerations

The crack growth rate and fatigue characteristics of the forgings were also extensively evaluated. Again, the data presented were primarily generated from the Boeing 747 Lower Link Fitting.

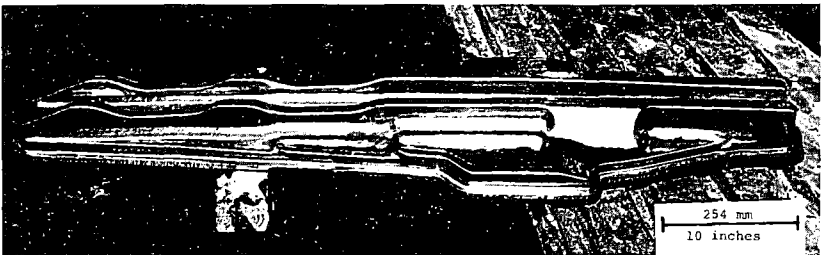


Figure 5a Conventionally forged Boeing 747 Lower Link Fitting made from Ti-10V-2Pe-3Al Alloy

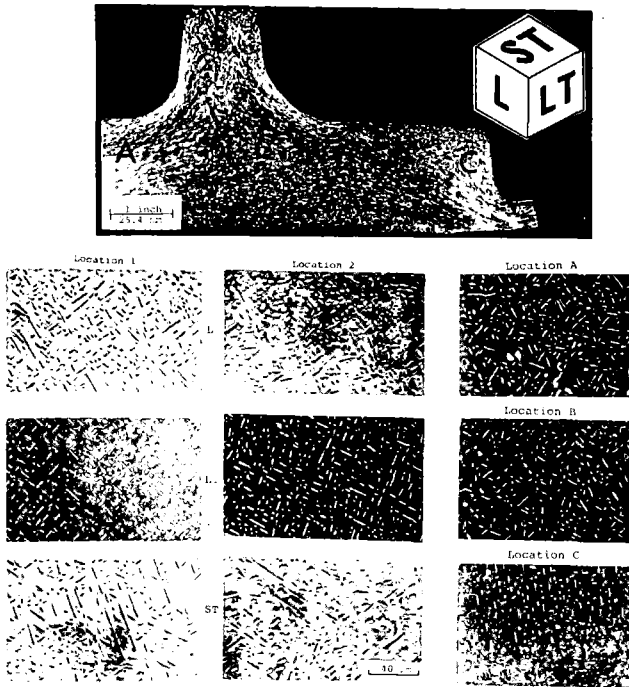
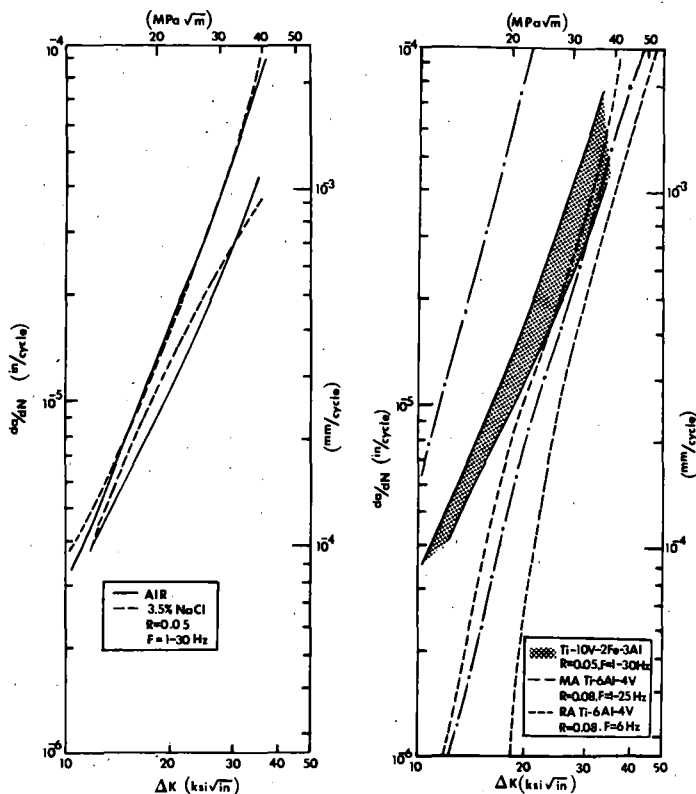


Figure 5b Typical macro- and microstructures of the Boeing 747 Lower Link Fitting forgings made from Ti-10V-2Fe-3Al alloy at high strength

The fatigue crack growth rate data for these Ti-10-2-3 forgings are presented in Figures 6a and 6b. The scatterbands in Figure 6a represent data collected in air and in 3.5% NaCl, tested at frequencies from 1-30 Hz in the L-S, T-L, L-T, and S-L orientations. No significant environmental effect was observed over the frequency ΔK ranges studied and no orientation effect could be discerned. The growth rates of Ti-10-2-3 are faster than recrystallized-annealed Ti-6-4 in the low ΔK regime and on the slower side of the mill annealed Ti-6-4 scatterband.

The Ti-10-2-3 alloy exhibits excellent high cycle fatigue behavior as illustrated in Figures 7 and 8. Fatigue strengths of about 965 MPa (140 ksi) are obtained at 10^6 cycles for the smooth specimens ($K_t=1$). As can be seen in Figure 7, this is a significant improvement over competitive titanium alloy materials in their more popular heat treatment conditions. This fatigue strength advantage is retained for notched specimens also. Above 10^4 cycles, the fatigue strength of Ti-6-4 and Corona-5 are clearly inferior to Ti-10-2-3.

Based on the above properties exhibited by the Ti-10-2-3 alloy obtained from forgings manufactured in production shops, the alloy has been demonstrated to be a viable alloy for aerospace structural applications. At the strength level discussed, the alloy offers weight savings of about 30% over Ti-6-4 and a theoretical 40% weight savings over steel at the same strength level, assuming the part is not stiffness critical. In the light of the increasing fuel costs and increased emphasis on structural efficiency, it should have a bright future for aerospace applications.



(a) Superimposed air and 3.5% NaCl fatigue crack propagation rate scatterbands for Ti-10V-2Fe-3Al at various orientations.
 (b) Comparison of fatigue crack growth rates of Ti-10V-2Fe-3Al to Ti-6Al-4V.

Figure 6 Fatigue crack growth rate data for high strength Ti-10V-2Fe-3Al Alloy

In addition to the structural efficiency of Ti-10-2-3, another advantage of the alloy is its forging characteristics. Using conventional forging practice, the alloy can be forged at lower temperatures and requires much less cleanup and surface reconditioning compared to commercial ($\alpha+\beta$) alloys such as Ti-6-4 or Ti-6Al-6V-2Sn. Ti-10-2-3 also appears to be an excellent alloy for hot die or isothermal forging. This forging can be accomplished in the 760C (1400F) temperature range, while Ti-6-4 is isothermally forged at about 954C (1750F). This difference in forging temperature results in significantly reduced tooling and forging costs, making the economics of isothermal forging much more attractive. In the light of the tight supply of titanium, isothermal forging should see increased applications in the future, and Ti-10-2-3 appears to be the most attractive titanium alloy for this technology.

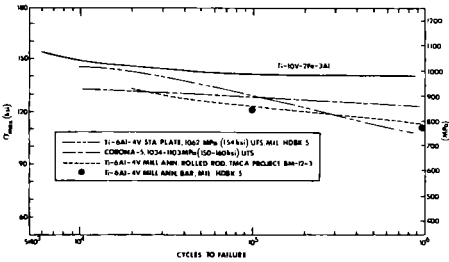


Fig. 7 Comparison of smooth fatigue strengths of Ti-10V-2Fe-3Al, Ti-6Al-4V, and Corona-5 alloys

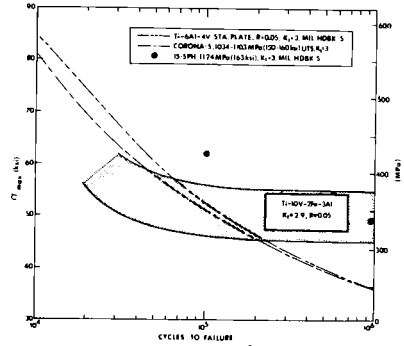


Fig. 8 Comparison of notched fatigue strengths of Ti-10V-2Fe-3Al, Ti-6Al-4V, Corona-5, and 15-5PH

Summary

The manufacturing methods for melting and those for forging, found to be necessary for producing high strength Ti-10-2-3 alloy forgings, have been determined. It was shown that, from a production standpoint, the achievable strength, ductility, and toughness properties at high strengths depend strongly on both the compositional homogeneity of the ingots and the forging and heat treating variables. Proper manipulation of the melting parameters are necessary to minimize both macro- and microsegregation making possible the restrictive avenues of thermomechanical processing necessary to achieve the desired balance of strength, toughness, and ductility.

References

1. "Metallurgical and Mechanical Properties of an Advanced High Toughness Alloy Ti-10V-2Fe-3Al", TIMET Titanium Data (Developmental), Titanium Metals Corporation of America, 1976.
2. W. Parris and H. W. Rosenberg: U.S. Patent 3,802,877, 4 April 1974.
3. E. Bohanek: Titanium Science and Technology, 3 (1973), 1993, Plenum Press, New York, 1973.
4. C. C. Chen and C. P. Gure: Wyman-Gordon Company Report RD-74-120, 1974.
5. C. C. Chen: Wyman-Gordon Company Report RD-75-118, 1975.
6. W. G. Pfann: Proceedings of the Seminar on Liquid Metals and Solidification, ASM Congress, November 1957, Chicago.
7. R. E. Adams and H. W. Rosenberg: Third International Conference on "Titanium", May 1976, Moscow, USSR.
8. H. W. Rosenberg and K. S. Snow: Light Metals, 1 (1973)
9. W. W. Tiller, et al: Acta Met, 1, (1953), 439.
10. C. C. Chen and R. R. Boyer: Journal of Metals, 31 (1979), 33.
11. C. C. Chen: Wyman-Gordon Company, Report RD-79-108, 1979.